A High-Resolution NMR Study of the La-Si-Al-O-N System

R. Dupree,* M. H. Lewis, and M. E. Smith

Contribution from the Department of Physics, University of Warwick, Coventry, CV4 7AL, U.K.
Received October 20, 1988

Abstract: High-resolution ^{27}Al, ^{29}Si, and ^{139}La NMR spectra have been obtained from crystalline phases of the La-Si-Al-O-N system. These results have further defined the ^{29}Si chemical shift ranges in mixed coordination tetrahedra (i.e., SiO_xN_{4-x}, $0 \leq x \leq 4$) and enabled the cation's influence on the chemical shift in such units to be investigated for the first time. The ability to distinguish distinct local environments, despite overlap of the ^{29}Si chemical shift ranges from different units, has allowed structural refinement of certain phases (e.g., $La_4Si_2O_7N_2$). The ^{27}Al NMR spectrum of $LaAlO_3$ shows appreciable intensity from transitions other than the $^1/_2 \leftrightarrow -^1/_2$, emphasing the difficulties of quantitatively interpreting NMR spectra of quadrupole nuclei. For the first time MAS is applied to ^{139}La NMR and is shown to have some limited applicability to the study of ceramics. High-resolution multinuclear NMR is shown to be a powerful monitor of phase development and probe of compositional detail in complex ceramic phase mixtures.

High-resolution solid-state NMR has provided important new structural information for inorganic materials. Variation in bonding changes the local electronic environment of the nuclei which results in small changes of the NMR frequency that are readily measured by applying high-resolution techniques such as magic angle spinning (MAS).[1] To date ^{29}Si (nuclear spin $I = {}^1/_2$) has been the most studied nucleus in inorganic systems, followed by ^{27}Al ($I = {}^5/_2$). NMR studies have been most valuable in materials where conventional techniques such as X-ray diffraction (XRD) can provide little information about the structure because of either the lack of long-range order or the similarity of the constituent element's scattering factors. NMR is principally concerned with short-range, local order and is element specific. The range of materials studied by both ^{29}Si and ^{27}Al NMR includes minerals,[2-4] zeolites,[5] phyllosilicates,[6,7] and amorphous materials.[8-10]

The isotropic chemical shift for both ^{29}Si and ^{27}Al has been shown to be influenced by a number of structural features, the most important being the local coordination, with the shift ranges of $(Si/Al)O_4$ units being easily resolvable from $(Si/Al)O_6$ units.[11] For SiO_4 tetrahedra empirical correlations of the resonance frequency to a number of factors including connectivity, next nearest neighbor, cation type, and bond length and bond angle have been published. For ^{27}Al, although AlO_4 and AlO_6 units can be distinguished, further interpretation is usually ambiguous as small changes of the chemical shift from structural alterations are convolved with the second-order quadrupole shift of the peak position of the ($^1/_2 \leftrightarrow -^1/_2$) transition away from the isotropic chemical shift.[12,13] In the case of quadrupolar nuclei in sites with sufficiently large electric field gradients, spectral intensity is lost owing to extreme broadening and incomplete excitation of even the central transition.[14,15]

The range of structural parameters investigated has recently been increased by the study of oxynitrides where both silicon and aluminum can have mixed (i.e., oxygen and nitrogen) nearest neighbor environments. Initially some sialon ceramic phases[16-18] were examined, followed by some Y-sialon glasses.[19] Chemical shifts for the complete range of tetrahedra SiO_xN_{4-x} ($0 \leq x \leq 4$) were first defined by examining the crystalline phases of the Y-Si-O-N system.[20] ^{29}Si and ^{27}Al NMR spectra from β'-sialon allowed a local structural model to be proposed even though the aluminum from mixed nearest neighbour units (i.e., AlO_3N, AlO_2N_2, and $ALON_3$) was broadened beyond detection.[21] Both ^{27}Al and ^{29}Si show a shift to higher frequency with increasing nitrogen content which is possibly related to the decrease in the electronegativity of the attached atom.

Study of the La-Si-Al-O-N system allows the cation influence on the ^{29}Si chemical shift of SiO_xN_{4-x} ($0 \leq x \leq 4$) units to be examined by comparison with the previous work on the Y-Si-O-N system as a number of isostructural phases are known to exist (e.g., $LaSiO_2N$, $La_4Si_2O_7N_2$, $La_5Si_3O_{12}N$). The local structure of a number of the La-Si-Al-O-N phases is not known, and it is shown here that high-resolution solid-state NMR can give information about the local atomic arrangement. The potential of high-resolution NMR to characterize complex ceramic mixtures has yet to be widely appreciated and some examples are highlighted.

Very little solid-state ^{139}La ($I = {}^7/_2$) NMR has been performed,[22,23] and its utility as a probe of these ceramics is examined. The quadrupole broadening of the ($^1/_2 \leftrightarrow -^1/_2$) transition is increased by a factor of $\sim$30 over ^{27}Al for sites with the same structural distortion in the same applied magnetic field, so that ^{139}La is expected to be observable in a more limited range of

(1) Andrew, E. R. *Int. Rev. Phys. Chem.* **1981**, *1*, 195-224.
(2) Smith, K. A.; Kirkpatrick, R. J.; Oldfield, E.; Henderson, D. M. *Am. Mineral* **1980**, *68*, 1206-1215.
(3) Kirkpatrick, R. J.; Smith, K. A.; Schramm, S.; Turner, G.; Yang, W. H. *Annu. Rev. Earth Planet. Sci.* **1985**, *13*, 29-47.
(4) Kinsey, R. A.; Kirkpatrick, R. J.; Hower, J.; Smith, K. A.; Oldfield, E. *Am. Mineral.* **1985**, *70*, 537-548.
(5) Kilinowski, J. *Prog. NMR Spectrosc.* **1984**, *16*, 237-309.
(6) Sanz, J.; Serratosa, J. M. *J. Am. Chem. Soc.* **1984**, *106*, 4790-4793.
(7) Weiss, C. A.; Altaner, S. P.; Kirkpatrick, R. J. *Am. Mineral.* **1987**, *72*, 935-942.
(8) Dupree, R.; Holland, D.; McMillan, P. W.; Pettifer, R. F. *J. Non-Cryst. Solids* **1984**, *68*, 399-410.
(9) Kirkpatrick, R. J.; Dunn, T.; Schramm, S.; Smith, K. A.; Oestrike, R.; Turner, G. In *Structure and Bonding in Non-Crystalline Solids*; Walrafen, G. E., Revesz, A. G., Eds.; Plenum Press: New York, 1986; pp 303-327.
(10) Dupree, R.; Holland, D.; Williams, D. S. *Phys. Chem. Glasses* **1985**, *26*, 50-52.
(11) Dupree, R.; Holland, D. In *New Horizons in Glass and Glass-Ceramics*; Lewis, M. H., Ed.; Chapman Hall: New York, 1989; Chapter I.
(12) Lippmaa, E.; Samoson, A.; Magi, M. *J. Am. Chem. Soc.* **1986**, *108*, 1730-1735.
(13) Muller, D.; Gessner, W.; Samoson, A.; Lippmaa, E.; Scheler, G. *J. Chem. Soc., Dalton Trans.* **1986**, 1277-1281.
(14) Muller, D.; Berger, G.; Grunze, I.; Ladwig, G.; Hallas, E.; Haubenreisser, U. *Phys. Chem. Glasses* **1983**, *24*, 37-42.
(15) Hallas, E.; Hahnert, M. *Cryst. Res. Technol.* **1985**, *20* K(25-28).
(16) Butler, N. D.; Dupree, R.; Lewis, M. H. *J. Mater. Sic. Lett.* **1984**, *3*, 469-470.
(17) Klinowski, J.; Thomas, J. M.; Thompson, D. P.; Korgul, P.; Jack, K. H.; Fyfe, C. A.; Gobbi, G. C. *Polyhedron* **1984**, *11*, 1267-1269.
(18) Dupree, R.; Lewis, M. H.; Leng-Ward, G.; Williams, D. S. *J. Mater. Sci. Lett.* **1985**, *4*, 561-564.
(19) Aujla. R. A.; Leng-Ward, G.; Lewis, M. H.; Seymour, E. F. W.; Styles, G. A.; West, G. W. *Phil. Mag. A* **1986**, *54*, L(51-56).
(20) Dupree, R.; Lewis, M. H.; Smith, M. E. *J. Am. Chem. Soc.* **1988**, *110*, 1083-1087.
(21) Dupree, R.; Lewis, M. H.; Smith, M. E. *J. Appl. Cryst.* **1988**, *21*, 109-116.
(22) Lutz, O.; Oehler, H. *J. Magn. Reson.* **1980**, *37*, 261-267.
(23) Thompson, A. R.; Oldfield, E. *J. Chem. Soc., Chem. Commun.* **1987**, 27-28.

0002-7863/89/1511-5125$01.50/0

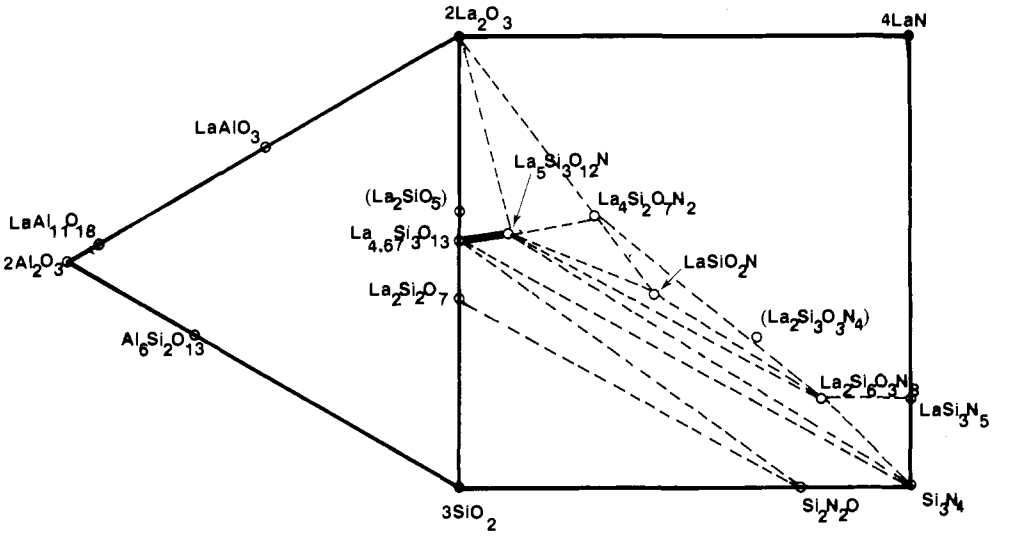

Figure 1. A behavior diagram for the La–Si–Al–O–N system showing the known crystalline phases.

compounds than ^{27}Al. Previously only static ^{139}La NMR spectra from some model inorganic compounds have been presented.[23]

The La–Si–Al–O–N System

The crystalline phases of the La–Si–Al–O–N system (Figure 1) and their relationships are much less well known than in the Y–Si–Al–O–N system. Only two aluminates are known to form, an almost cubic perovskite $LaAlO_3$ and a β-alumina ($LaAl_{11}O_{18}$), both of which are stable from their melting points to room temperature,[24] compared with the three yttrium aluminates with compositions 2:1 (Y_2O_3:Al_2O_3), 1:1, and 3:5. La_2O_3–SiO_2 phase diagrams show three crystalline silicates at 1:1 (La_2O_3:SiO_2), ~2:3 and 1:2,[25] although it has been claimed that La_2SiO_5 does not form.[26] The ~2:3 compound is more accurately described as $La_{4.67}Si_3O_{12-13}$, an extension of the *N*-apatite ($La_5Si_3O_{12}N$) solid solution to the silicate phase boundary, which does not occur for yttrium. The disilicate has two polymorphs with the low-temperature[1] tetragonal form transforming above 1275 °C to the high-temperature (h) orthorhombic form.[27] The phase behavior along the La_2O_3–Si_3N_4 boundary has remained uncertain, in particular whether or not *N*-melilite ($La_2Si_3O_3N_4$) exists. Initial studies suggested that $La_2Si_3O_3N_4$ did form,[28,29] although the XRD pattern was very similar to $LaSiO_2N$.[28] More recently it was claimed that the 1:1 (La_2O_3:Si_3N_4) composition melts at ~1650 °C producing a mixture of phases but no *N*-melilite.[30] A new stable compound forms at $1La_2O_3$:$2Si_3N_4$ which is unknown in the yttrium system. Little is known about this phase except that it indexes on a monoclinic unit cell[30] with no information about the local structure since, unlike most other oxynitrides, no mineral analogue exists. In addition a sole nitride, $LaSi_3N_5$, has been synthesized.[31]

Experimental Section

The crystalline phases were prepared by solid-state sintering stoichiometric mixtures of pure (>99.9%) La_2O_3, SiO_2, α-Al_2O_3, Si_3N_4, and LaN powders. LaN and La_2O_3 were handled under a dry nitrogen atmosphere to prevent their reaction with moisture which is particularly rapid for LaN. The powders were dry mixed, pelletized, and embedded in pure BN powder in graphite crucibles. The samples were heated to 1550–1775 °C in a graphite susceptor induction furnace for ~2 h under a flow of oxygen-free nitrogen. All samples were characterized for mass loss, by XRD and some by scanning electron microscopy.

The MAS–NMR was performed at 50.9 MHz (^{139}La), 71.535 MHz (^{29}Si), and 93.83 MHz (^{27}Al) on a Bruker MSL-360 spectrometer. ^{29}Si spectra were accumulated using small pulse angles ~15° combined with pulse delays of ~60 s to maximize signal-to-noise, although the long ^{29}Si spin–lattice relaxation time (T_1 ~ hours in some samples) may result in quantitative detail on the phase distribution being lost. Short (~1 μs), intense (B_1 ~ 5 mT) pulses were used on ^{27}Al and ^{139}La to excite the spectrum as completely as possible and prevent distortion of the line shape due to quadrupole nutation, with 1–10-s delays between the pulses. The intensity of ^{27}Al spectra were integrated and compared to reagent grade

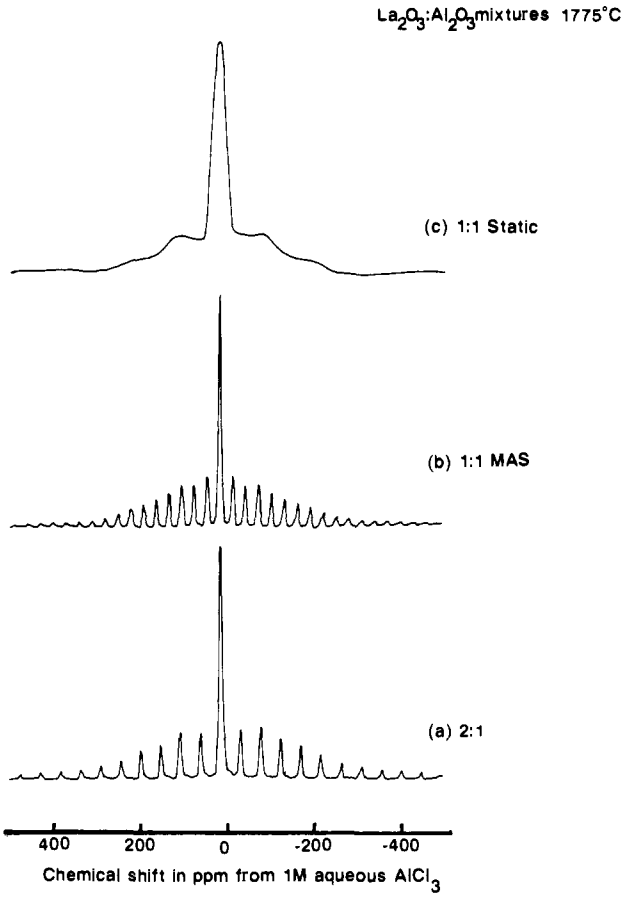

Figure 2. ^{27}Al NMR spectra of La_2O_3:Al_2O_3 mixtures sintered at 1775 °C for 2 h: (a) 2:1 MAS, (b) 1:1 MAS, and (c) 1:1 static.

(24) Bondar, I. A.; Vinogradova, N. V. *Figure* 2340 in *Phase Diagrams for Ceramists*; Levin, E. M., Robbins, C. E., McMurdie, H. F., Eds.; American *Ceramic Society*: Columbus, OH, 1969.
(25) Figure 2372 in ref 24.
(26) Kuimin, E. A.; Belov, N. V. *Sov. Phys. Dokl.* **1966**, *10*, 1009–1011.
(27) Felsche, J. *Struct. Bonding* **1973**, *13*, 99–198.
(28) Wills, R.; Stewart, R. W.; Cunningham, J. A.; Wimmer, J. M. *J. Mater. Sci.* **1976**, *11*, 749–759.
(29) Marchand, R.; Jayaweera, A.; Verdier, P.; Lang, J. *C. R. Acad. Sci. Paris* **1976**, *C385*, 675–677.
(30) Mitomo, M.; Izumi, F., horruchi, S.; Matsui, Y. *J. Mater. Sci.* **1982**, *17*, 2359–2364.
(31) Inoue, Z.; Mitomo, M. T.; Nobou, I. *J. Mater. Sci.* **1980**, *15*, 2915–2920.

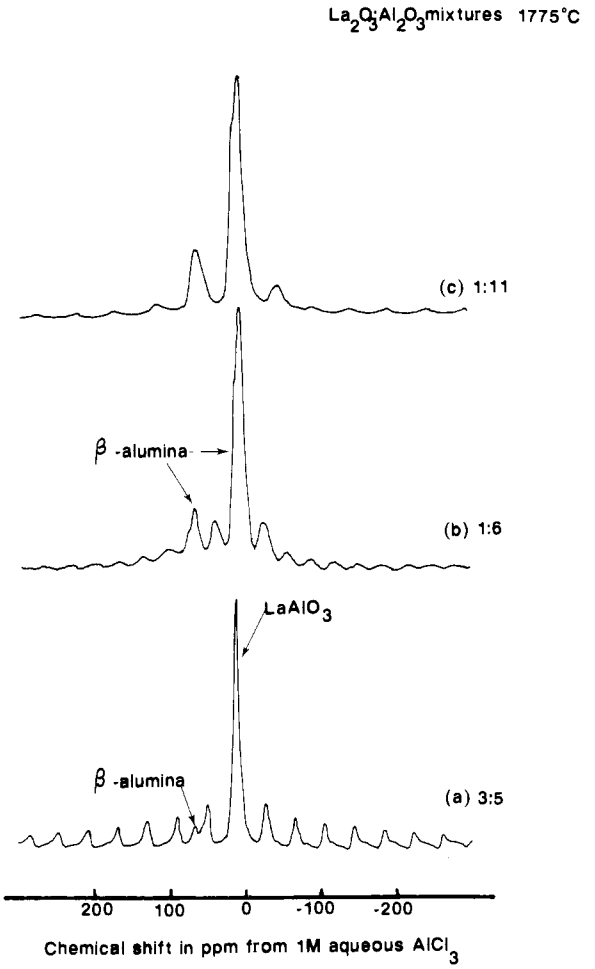

Figure 3. ^{27}Al MAS-NMR spectra of La_2O_3:Al_2O_3 mixtures sintered at 1775 °C for 2 h: (a) 3:5, (b) 1:6, and (c) 1:11.

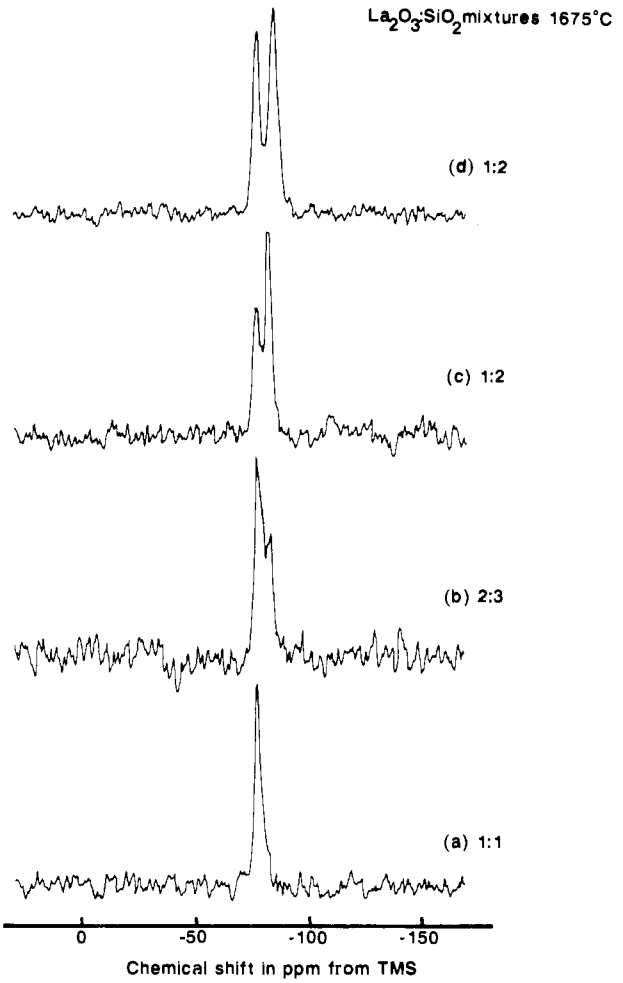

Figure 4. ^{29}Si MAS-NMR spectra of La_2O_3:SiO_2 mixtures sintered at 1675 °C for 2 h: (a) 1:1, (b) 2:3, (c) 1:2, and (d) 1:2.

α-Al_2O_3 to allow quantification of the fraction of ^{27}Al detected in the experiment. To obtain static ^{139}La spectra, a quadrupole echo sequence ($90_{\pm x} - \tau - 90°_{y} - \tau' - (Acq)_{\pm x}$ using pulses which are 90° on the $^1/_2 \leftrightarrow -^1/_2$ transition for nuclei in sites with large electric field gradients) was used to overcome probe ringing effects that cause distortions of the spectrum.[32] The samples were finely powdered and ~0.5 g was packed in conventional Andrew-type spinners and spun at 3-4.5 kHz. Data processing involved 0-100 Hz exponential smoothing to improve the signal-to-noise. All spectra were externally referenced to either 1 M aqueous $AlCl_3$ (^{27}Al), Me_4Si (^{29}Si), or 1 M aqueous $La(NO_3)_3$ (^{139}La).

NMR Spectroscopy

^{27}Al NMR. A series of compositions (La_2O_3:Al_2O_3) were made to allow comparison with the Y_2O_3-Al_2O_3 system. All sinterings at 1775 °C produced only the two known phases whose relative content changed with composition as expected (Figures 2 and 3). It is informative to compare XRD and MAS-NMR analysis of these products since the differing aspect measured by each technique has to be carefully taken into account. XRD depends on the structure factor which is dominated by the heavy, large Z (atomic number) elements (e.g., lanthanum). $LaAlO_3$ and $LaAl_{11}O_{18}$ each have one lanthanum per formula unit so that XRD may give a reasonable measure of the amount of each phase present. However, the intensity of ^{27}Al NMR depends on the aluminum content which is much higher for the β-alumina. For the La_2O_3:$6Al_2O_3$ mixture, XRD indicates approximately $1LaAlO_3$:$1LaAl_{11}O_{18}$ as expected from its stoichiometry midway between the two compositions. ^{27}Al MAS-NMR (Figure 3b) is completely dominated by the β-Alumina and $LaAlO_3$ cannot be resolved, demonstrating that, if the elemental concentration of the phases is markedly different, the phase content could be incorrectly determined.

The aluminum coordination in $LaAlO_3$ is clearly octahedral from the shift (11.7-ppm peak position). The near-cubic symmetry of the structure is reflected in the symmetric local environment of aluminum which experiences only a small electric field gradient (efg). Other broadening mechanisms obscure the second-order quadrupole structure of the central transition, but the efg is sufficiently small that the first-order powder pattern of the higher order transitions (e.g., $^3/_2 \leftrightarrow {}^1/_2$) can be seen in the static spectrum (Figure 2c). The quadrupole interaction strength can be estimated from the higher order transitions as $e^2qQ/h \simeq (0.12 \pm 0.02)$ MHz with the accuracy being limited by the other broadenings which smooth the quadrupole line shape. This value agrees with a previous single-crystal measurement.[33]

$LaAl_{11}O_{18}$ gives two ^{27}Al resonances, at 8.5 and 66 ppm. The peak associated with octahedral coordination (8.5 ppm) has some structure although it is difficult to attribute, as it could either be due to second-order quadrupole effects or slight shifts in peak position of the different AlO_6 sites present. Integration of the spectrum gives (AlO_6/AlO_4) ~ 5.0 ± 0.7 which can be compared to 4.3 for the crystal structure.

^{29}Si NMR. Attempts to sinter La_2SiO_5 in the range 1600-1700 °C always resulted in a mixture of La_2O_3 and the apatite-structured silicate (Figure 4a). Apatite and disilicate compositions gave phase mixtures with the dominant phase changing as expected with composition (Figure 4b,c). At 1675 °C h-$La_2Si_2O_7$ should form, but one sintering unexpectedly produced the l-form which was confirmed by XRD and the change in isotropic chemical shift (Table I, Figure 4d). The shift of h-$La_2Si_2O_7$ is in agreement with a previous study.[34a]

(32) Gerothanassis, I. P. *Prog. NMR. Spectrosc.* **1987**, *19*, 267-329.

(33) Muller, K. A.; Burn, G.; Derighetti, B.; Drumheller, J. G.; Waldner, F. *Phys. Lett.* **1964**, *9*, 223-224.

Table I. ^{29}Si Isotropic Chemical Shifts, Line Widths, and Proposed Local Structural Units of the Crystalline Compounds of the La-Si-O-N System

compound	local silicon structural unit	^{29}Si isotropic chemical shift[a] ±0.5, ppm	fwhm ± 10%, fwhm, Hz
h-$La_2Si_2O_7$	SiO_4, $Q^{(1)}$	−82.6	230
l-$La_2Si_2O_7$	SiO_4, $Q^{(1)}$	−84.7	280
$La_{4.67}Si_3O_{12-13}$	SiO_4, $Q^{(1)}$	−77.7	200
$La_5Si_3O_{12}N$	SiO_4, $Q^{(1)}$	−77.7	200
$La_4Si_2O_7N_2$	SiO_3N, $Q^{(1)}$	−84.2	220
$LaSiO_2N$	SiO_2N_2, $Q^{(2)}$	−72.4	160
$La_2Si_6O_3N_8$	$SiON_3$,	−56.5	350
Si_2N_2O	$SiON_3$, $Q^{(7)}$	−61.9	120
$LaSi_3N_5$	SiN_4, $Q^{(7),(6)}$	−64.6	120
β-Si_3N_4	SiN_4, $Q^{(8)}$	−48.6	100

[a] With respect to Me_4Si.

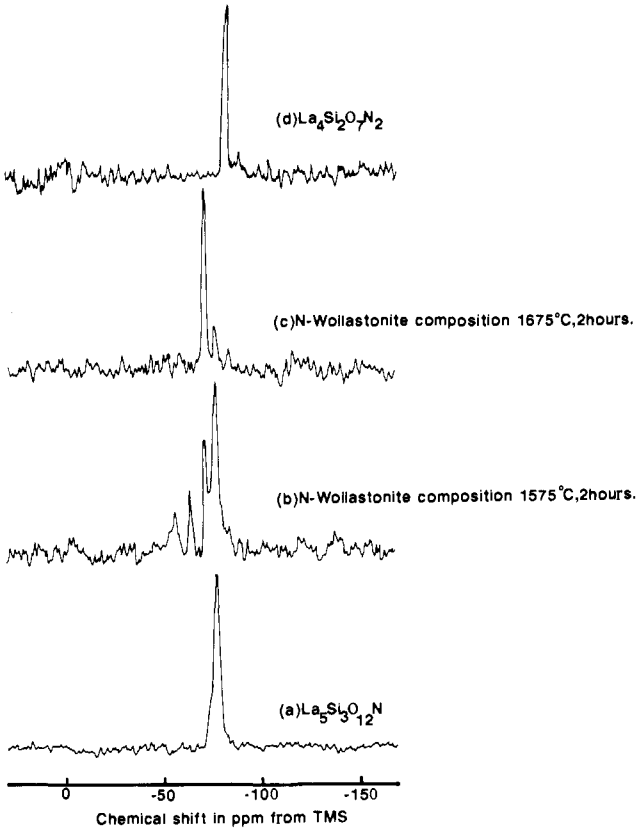

Figure 5. ^{29}Si MAS-NMR spectra of (a) $La_5Si_3O_{12}N$, *N*-wollastonite composition sintered at (b) 1575 °C, 2 h, (c) 1675 °C, 2 h, and (d) $La_4Si_2O_7N_2$.

Lanthanum *N*-apatite was readily prepared as a single phase unlike the yttrium analogue where a phase mixture with Y_2SiO_5 always formed.[20] It is expected that both SiO_4 and SiO_3N tetrahedra should be present in $La_5Si_3O_{12}N$, and, although two resonances are not immediately apparent, careful examination of the main resonance at −77.7 ppm reveals a positively shifted shoulder (Figure 5a) which is reproducible and is absent from the pure silicate apatite. The main resonance is attributed to SiO_4 units since it does not shift across the solid solution and the shoulder is assigned to SiO_3N units.

The phase development of $LaSiO_2N$ can clearly be followed by the MAS-NMR spectra (Figure 5b,c). After 2 h at 1575 °C XRD indentifies only $LaSiO_2N$ and *N*-apatite. NMR shows four resonances at −56.5, −64.6, −72.4, and −77.7 ppm (Figure 5b). "Fingerprinting" this spectrum using Table I allows all these peaks to be readily identified. Increasing the sintering temperature to

(34) (a) Mitteilung, K.; Grimmer, A.-R.; Lampe, F. V.; Magi, M.; Lippmaa, E. *Monatsh. Chem.* **1983**, *114*, 1053-1057. (b) Harris, R. K.; Leach, M. J.; Thompson, D. P., to be published.

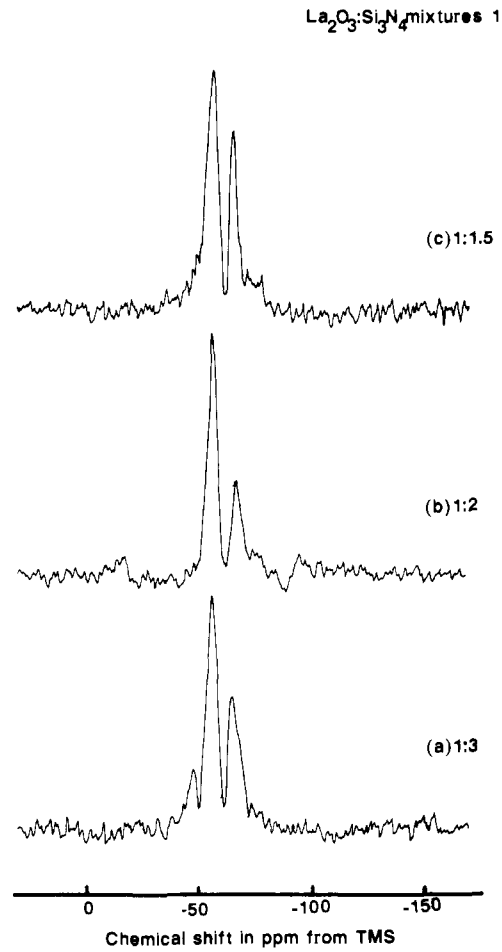

Figure 6. ^{29}Si MAS-NMR spectra of La_2O_3:Si_3N_4 mixtures sintered at 1675 °C for 2 h: (a) 1:3, (b) 1:2, and (c) 1:1.5.

1675 °C produced almost single-phase *N*-wollastonite after 2 h. XRD showed only *N*-wollastonite which is assigned to the dominant NMR peak at −72.4 ppm, and the minor peak at −77.7 ppm is consistent with some residual apatite phase that was not detected by XRD. Single-phase $La_4Si_2O_7N_2$ readily formed after 2 h at 1550 °C with only a single resonance at −84.2 ppm (Figure 5d).

Various mixtures of Si_3N_4 and La_2O_3 were sintered at 1675 °C with the results shown in Figures 6 and 7. Throughout the composition range 1:3 (La_2O_3:Si_3N_4) to 1:1.5 two strong resonances are apparent at −56.5 and −64.6 ppm with the 1:3 composition showing some unreacted Si_3N_4 at −49 ppm. The peaks at −56.5 and −64.6 ppm are identified with $La_2Si_6O_3N_8$ and $LaSi_3oN_5$, respectively (Table I), even though XRD could not detect $LaSi_3N_5$. It should be noted that NMR, which is sensitive to only short-range effects in a sample, can often detected phases that XRD cannot, owing to unfavorable X-ray structure factors or the degree of crystallinity of the phase. Recent work by Harris et al.[34b] suggests that $La_2Si_6O_3N_8$ has two resonances at −57.3 and −68.2 ppm in the ratio 3:1. It is possible the −68.2-ppm resonance is present in our samples but is obscured by impurity $LaSi_3N_5$. The 1:1 composition produced complex phase mixtures with an abrupt change about its melting temperature of ~1650 °C (Figure 7a,b). Below the melting point the most prominent peak is at −64.6 ppm with minor resonances at −56.5, −72.4, and −77.7 ppm. The dominant XRD lines from this specimen correspond to *N*-wollastonite which may explain why the original work on this composition identified a crystalline phase with a similar XRD pattern to $LaSiO_2N$. Above ~1650 °C a more complicated NMR spectrum is observed with some of the peaks having shifted close to β-Si_3N_4, $La_2Si_6O_3N_8$, and $La_5Si_3O_{12}N$. However, as the isotropic chemical shifts and line widths cannot be exactly matched, these phases are not thought to be present. A complex XRD pattern is also obtained with numerous unas-

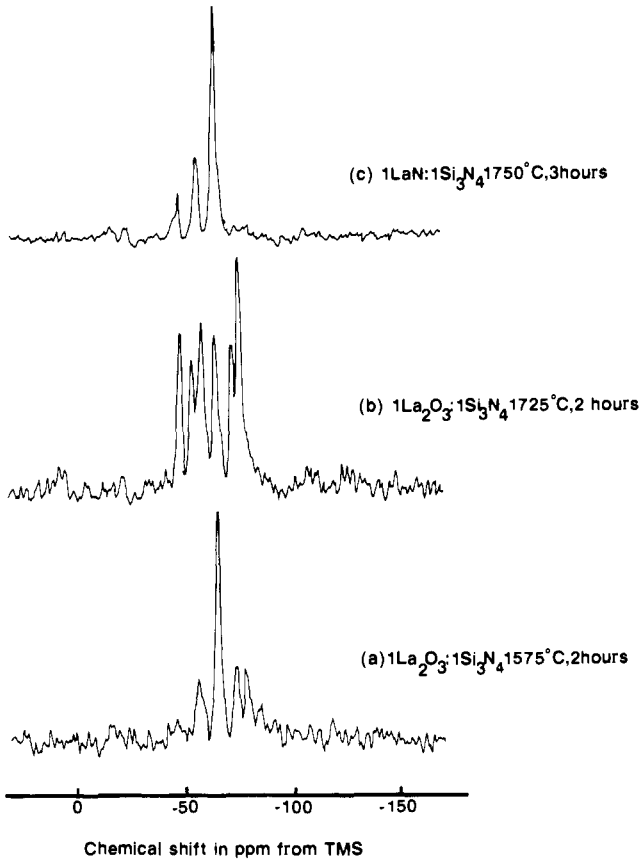

Figure 7. ^{29}Si MAS-NMR spectra of the *N*-melilite composition sintered (a) below the melting point and (b) above the melting point. (c) $LaN:Si_3N_4$ sintered at 1750 °C for 2 h.

signable lines, and this structure is ascribed to a range of metastable phases which may have formed from the melt.

A mixture of $1LaN:1Si_3N_4$ sintered at 1750 °C for 3 h produced $LaSi_3N_5$ as the major phase corresponding to the peak at −64.6 ppm (Figure 7c). The two other peaks correspond to unreacted Si_3N_4 and $La_2Si_6O_3N_8$ which is not unexpected as oxygen contamination of LaN is difficult to avoid, and the La_2O_3–Si_3N_4 mixtures showed $LaSi_3N_5$ and $La_2Si_6O_8N_8$ often occur together.

^{139}La NMR. Static spectra were initially accumulated on a number of samples using a quadrupole echo sequence. Both La_2O_3 and $LaAl_{11}O_{18}$ produced short-lived echoes (a few microseconds) corresponding to very broad resonances covering several hundred kilohertz which are of limited use in trying to understand structure. This agrees with their known local structures, as La_2O_3 contains lanthanum in a distorted seven-coordinate environment and the β-alumina is surrounded by oxygens at varying bond lengths, so that large efg's are expected. Hence, phases where lanthanum has both oxygen and nitrogen nearest neighbors were not examined as large efg's were also anticipated.[21] The only phase which produced unambiguous results was $LaAlO_3$ where lanthanum is in a symmetric LaO_{12} local coordination. The static line was sufficiently narrow not to require an echo and it produced a recognizable second-order quadrupole line shape (Figure 8b) which readily narrows on spinning (Figure 8a). Fitting the line shape allows both the isotropic chemical shift (375 ± 5 ppm) and the quadrupole coupling constant ($e^2qQ/h \sim 6$ MHz) to be calculated. The lack of any shoulders on the line shape and the narrowing factor of ~3.7 (static → spinning) suggests a quadrupole asymmetry parameter of ~0. Figure 8c illustrates that great care has to be exercised in solid-state studies of quadrupole nuclei as a pulse of only 3 μs ($\sim\pi/8$ on a liquid) completely distorts the line shape. This is in agreement with calculations of the effect of quadrupole nutation of the magnetization during the rf pulse.[35-37]

(35) Samoson, A.; Lippmaa, E. *Phys. Rev. B.* **1983**, *23*, 6567–6570.

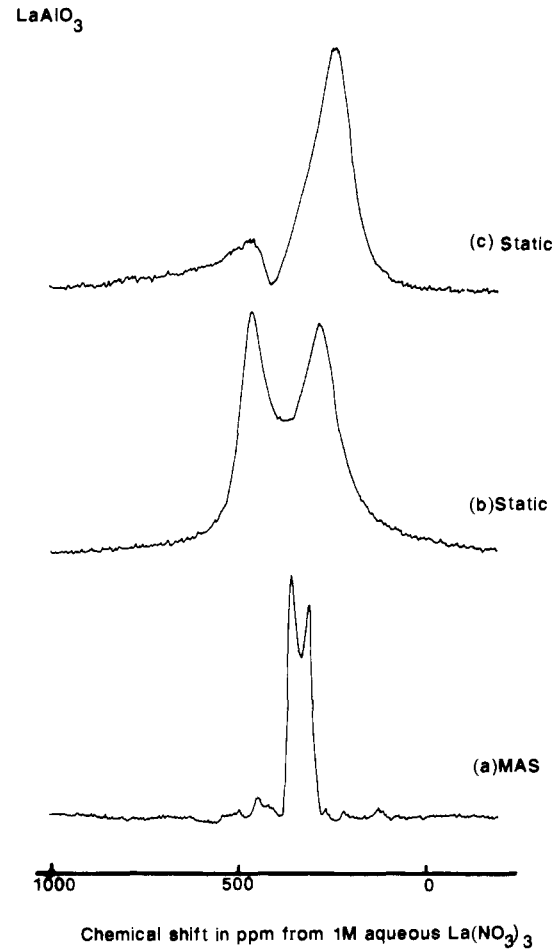

Figure 8. ^{139}La NMR spectra of $LaAlO_3$: (a) MAS, (b) static with a 1-μs rf pulse, and (c) static with a 3-μs rf pulse (B_1 = 5 mT).

Discussion

^{27}Al Chemical Shifts. The well-separated shift ranges of AlO_4 and AlO_6 units allow rapid identification of the coordinations present in these phases. $LaAlO_3$ contains aluminum in a regular octahedral environment while the hexagonal β-alumina has a magnetoplumbite structure which is based on spinel-like blocks consisting of edge-sharing AlO_6 octahedra interconnected by AlO_4 tetrahedra. Single-crystal XRD studies have shown that there are three distinct AlO_6 environments and that the structural blocks are interconnected by AlO_5 units (~2 per unit cell). It is variation of the occupancy of these AlO_5 sites which results in a range of compositions of this compound.[38] Observation of subtle distinctions in the local environment, such as those between the AlO_6 units in the β-alumina, are complicated by the second-order quadrupole shift of the peak position away from the isotropic chemical shift and are obscured by the residual quadrupole broadening. The ^{27}Al NMR peak positions of the AlO_6 corner-sharing in $LaAlO_3$ (11.7 ppm) and edge-sharing in $LaAl_{11}O_{18}$ (~8 ppm) are different, but because of the quadrupole effects the use of ^{27}Al MAS NMR spectra alone at one magnetic field to distinguish local structural models is unwise.

Quantification of Quadrupole Perturbed NMR Spectra. The quantitative aspect of pulsed NMR spectra has to be carefully considered when dealing with broad resonances, such as encountered with quadrupole nuclei. It is important to establish which transitions are being observed in the spectrum and to what

(36) Fenkze, D.; Freude, d.; Frohlich, T.; Haase, J. *Chem. Phys. Lett.* **1984**, *111*, 171–175.
(37) Geurts, F. M. M.; Kentgens, A. P. M.; Veeman, W. S. *Chem. Phys. Lett.* **1985**, *120*, 206–210.
(38) Iyi, N.; Inoue, Z.; Takekawa, S.; Kimura, S. *J. Solid State Chem.* **1984**, *54*, 70–77.

extent spectral intensity is being lost. To excite the spectrum as completely as possible and prevent spectral distortion, only short, intense rf pulses (corresponding to small pulse angles) should be used.[12,35,36,39]

The small efg at the aluminum site in $LaAlO_3$ leads to considerable higher order transition intensity being present, whereas for the β-alumina essentially only the $(^1/_2 \leftrightarrow -^1/_2)$ transition is observed. This can be seen by comparison with the integrated intensity to α-Al_2O_3 of 1.9 for $LaAlO_3$ and 1.1 for $LaAl_{11}O_{18}$. Any attempt to quantitatively use the NMR spectrum to describe a phase mixture of these two phases would be in serious error if the differing contributions of the transitions were not accounted for. In $LaAlO_3$ the integrated intensity ratio of the higher order transitions/central transition is $\sim 5/3$, less than the theoretical ratio of ~ 3. This agrees with the expected greater loss of intensity from the first-order quadrupole perturbed transitions compared with the second-order quadrupole perturbed central transition.

For β-alumina the high value of the AlO_6/AlO_4 ratio obtained from the NMR spectrum further illustrates the difficulties associated with quantitative interpretation. This result may be explained as higher order transition sidebands associated with the octahedral site are observed, indicating a smaller efg, so that the octahedral center band will have less intensity loss than the tetrahedral site. Also the AlO_5 units may have efg's such that their intensity is second-order quadrupole shifted into the AlO_6 shift range (cf. andalusite[40]). As the AlO_5 resonance cannot be observed, the different structural models for the β-alumina which depend on the occupancy of this site cannot be distinguished.

Structural Models for La–Si–O–N Compounds. As for the yttrium compounds, little work has been performed to elucidate the local order of oxygen and nitrogen in La–Si–O–N compounds. Understanding of their likely position has been enhanced by application of Pauling's second crystal rule to oxynitride structures.[41,42] The general trend shown by this work is nitrogen, which tries to have a bond order sum as close to 3 as possible, tends to coordinate to as many silicons as allowed by the structure. MAS–NMR can distinguish different local environments in these materials which tests these ideas. $LaSiO_2N$ provides a useful standard since single-crystal XRD studies have established the local silicon environment as being made up of rings of three SiO_2N_2 tetrahedra connected via bridging nitrogens.[43] MAS–NMR shows a single resonance with no structure, consistent with a single silicon environment. In the phases $La_2Si_6O_3N_8$, $La_5Si_3O_{12}N$, and $La_4Si_2O_7N_2$ the local silicon environment is less certain.

$La_4Si_2O_7N_2$ contains isolated $Si_2O_5N_2$ units, and the question is whether nitrogen occupies the bridging position (see ref 20). Bond-order arguments suggest that, although the bridging position is most suitable for nitrogen substitution, the nonbridging positions are also possible substitution sites.[42] For $Y_4Si_2O_7N_2$ it has been shown that nitrogen does not occur in the bridging position as only one NMR resonance was observed,[20] and a nitrogen in the bridging position requires both SiO_2N_2 and SiO_3N tetrahedra leading to two resonances. For $Y_4Si_2O_7N_2$ a neutron diffraction study also only found SiO_3N units.[44] For $La_4Si_2O_7N_2$ no previous work on the local structure has been performed. Again only one resonance of comparable width to $LaSiO_2N$ is found indicative of a single SiO_3N environment.

In *N*-apatite the local silicon environments are dominated by isolated SiO_4 units; this is simply seen by the constancy of the shift of the main peak, even in the pure silicate apatite. A high-frequency shoulder in the $La_5Si_3O_{12}N$ composition is attributed to isolated SiO_3N units which are expected, although some doubt has recently been case as to whether $La_5Si_3O_{12}N$ forms.[34b] *N*-Apatite and $La_4Si_2O_7N_2$ have mineral analogues $Ca_5(PO_4)_3F$ and $Ca_4Si_2O_7F_2$, respectively, and the MAS–NMR results clearly confirm the bond-strength ideas that nitrogen does not simply replace fluorine but bonds to silicon to satisfy its bond-order requirements.

The nitride $LaSi_3N_5$ contains SiN_4 tetrahedra that are linked in five-membered rings about lanthanum ions according to the crystal structure derived by a single-crystal XRD study.[31] These tetrahedra have from one to three nitrogens with nonbridging bonds to the lanthanum (i.e., $N^{-}\cdots{}^{+}La$). In crystalline silicates SiO_4 tetrahedra with differing numbers of nonbridging bonds are normally distinguishable. However, $LaSi_3N_5$ produces only one narrow resonance; hence MAS–NMR is unable to distinguish supposedly different silicon sites in this crystal structure. The distinction between bridging and nonbridging nitrogens is less clear than for oxygen, as nitrogen is trivalent, rather than divalent, so that it can have a nonbridging bond yet still be connecting two silicons. This suggests that influence of nonbridging bonds of nitrogen on the ^{29}Si chemical shift is less marked than for oxygen.

The single resonance from $La_2Si_6O_3N_8$ is indicative of a single silicon environment. From the composition the most likely unit is $SiON_3$, although this cannot be unambiguously proved from the MAS–NMR spectrum. If this phase has two resonances[34b] at -57.3 and -68.2 ppm, it is likely that the corresponding units are SiO_3N and SiO_2N_2, respectively.

^{29}Si Chemical Shift Ranges of SiO_xN_{4-x} Units. The lanthanum compounds studied in this research have extended the number of shifts measured for SiO_xN_{4-x} ($0 \le x \le 4$) tetrahedra. Together with previous measurements on the Y–Si–O–N system, a more complete idea of the chemical shift ranges of these units is obtained. The trend to more positive shifts with increasing nitrogen content is clear (Figure 9). This agrees with an increasing paramagnetic shift as the average covalency of the bonds increases on replacing oxygen with nitrogen. However, as was found for SiO_4 groups with an increasing data base, the different units have shift ranges with considerable overlap so that a local structural unit cannot be unambiguously identified from its shift position. This is illustrated by considering a shift of ~ 65 ppm where materials containing SiN_4, $SiON_3$, SiO_2N_2, and SiO_3N have all recorded resonances in these two systems (Figure 9).

For silicates the completely connected SiO_4 tetrahedron gives the most negative shift, and the presence of any nonbridging bonds usually makes the shift more positive. Yet even in the small selection of compounds based solely on SiN_4 units studied so far, $Y_2Si_3N_6$[45] and $LaSi_3N_5$ show marked negative shifts compared with the fully connected Si_3N_4 which is still unexplained.

Comparison of the Lanthanum and Yttrium Systems. The relative stability of certain compounds clearly changes in going from the yttrium system to the lanthanum one. $(Y/La)_4Si_2O_7N_2$ is the most stable compound in both systems as it forms as a single phase at relatively low temperatures (~ 1550 °C) and shows no sign of decomposition in the temperature range 1550–1700 °C. *N*-Apatite is also stable in both systems, but for lanthanum it appears to be stable throughout a composition range to the pure silicate phase boundary. The stability of *N*-wollastonite clearly changes between the two systems being stable between 1550 and 1700 °C in the lanthanum system, while for yttrium, above ~ 1500 °C, it decomposes to Si_3N_4 and $Y_4Si_2O_7N_2$. Our results convincingly show that between ~ 1500 and 1700 °C no *N*-melilite phase forms in the lanthanum system, but the $2Si_3N_4{:}1La_2O_3$ compound does in agreement with a previous phase study.[30] It is also interesting to note that at the *N*-melilite composition $(Y,La)Si_3N_5$ forms during the early phase of development which has not previously been reported. The relative stability of oxynitrides and aluminates which form clearly depends on the size of the cation.

The ^{29}Si line widths for silicon sites in the Y–Si–O–N system with only oxygen nearest neighbors are generally narrower than

(39) Man, P. P.; Klinowski, J.; Trokiner, A.; Zanni, H.; Papan, P. *Chem. Phys. Lett.* **1988**, *151*, 143.
(40) Alemany, L. B.; Kirker, G. W. *J. Am. Chem. Soc.* **1986**, *108*, 6158–6162.
(41) Morgan, P. E. D. *J. Mater. Sci. Lett.* **1986**, *5*, 372.
(42) Morgan, P. E. D. *J. Mater. Sci.* **1986**, *21*, 4305–4309.
(43) Morgan, P. E. D.; Carroll, P. J.; Lange, F. F. *Mater. Res. Bull.* **1977**, *12*, 251–260.
(44) Roult, R.; Bacher, P.; Liebaut, G.; Marchand, R.; Goursat, P.; Laurent, Y. *Acta Crystallogr.* **1984**, *A40* (Suppl.), C226.
(45) Smith, M. E. Ph.D. Thesis, University of Warwick, 1988.

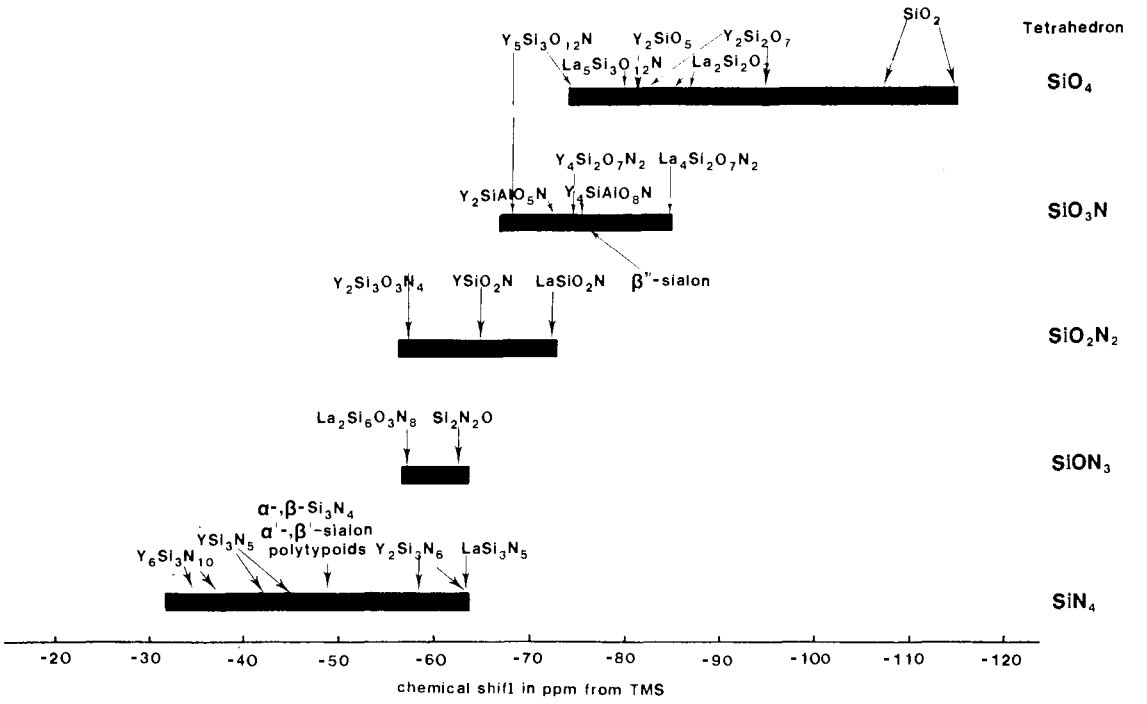

Figure 9. ^{29}Si isotropic chemical shift ranges for SiO_xN_{4-x} ($0 \leq x \leq 4$) tetrahedra from the (Y,La)–Si–Al–O–N systems.

for mixed environments,[20] essentially because oxygen possesses no magnetic dipole moment to cause any broadening. In MAS experiments, residual line widths may be attributed to a number of sources including variations in the local environment (i.e., crystallinity), and when silicon is bonded to ^{14}N ($I = 1$) the quadrupole nature of nitrogen may prevent complete averaging of the Si–N dipolar coupling.[46] For the yttrium system this distinction is clearly observed (fwhm: γ-$Y_2Si_2O_7 \simeq 50$ Hz; $Y_4Si_2O_7N_2 \simeq 320$ Hz),[20] whereas it is much less clear for the lanthanum system. Comparison of the disilicate ^{29}Si line widths from the two systems, which are of comparable crystallinity according to XRD, highlights this. The lanthanum disilicates are a factor 4–5 times broader than the yttrium disilicates which is most probably due to unaveraged La–Si dipolar coupling since lanthanum has a large quadrupole moment unlike the spin-$^1/_2$ yttrium.

Another interesting trend is seen from differences in the isotropic ^{29}Si chemical shift between nominally isostructural materials in both systems (Figure 10). The lanthanum materials are always negatively shifted by 4–10 ppm from the yttrium analogues. For silicates, bond strength–electronegativity arguments have been developed by considering the structural fragments (Si—O···M).[47] As the O···M bond becomes more ionic (i.e., M becomes less electronegative), the Si–O bond becomes more covalent and the ^{29}Si chemical shift more paramagnetic. This has been demonstrated by the reciprocity of the ^{29}Si and ^{89}Y shifts for yttrium silicates.[48] Lanthanum has a lower Pauling electronegativity (1.1) than yttrium (1.2), so, that more positive ^{29}Si chemical shifts would be expected for the lanthanum system. This is demonstrably not the case, indicating that structural factors other than straightforward electronegativity effects are determining the chemical shift.

Conclusion

^{29}Si MAS–NMR has been shown to be an effective method for investigating silicon oxynitrides. The number of measured ^{29}Si shifts for all tetrahedra SiO_xN_{4-x} ($0 \leq x \leq 4$) has been increased, and a trend to more positive chemical shift with increasing nitrogen content is clearly shown. Despite extensive overlap of the different chemical shift ranges, NMR spectra have allowed refinement of the local atomic structure of $La_4Si_2O_7N_2$ and $La_5Si_3O_{12}N$. The lanthanum compounds consistently show a more negative shift than the isostructural yttrium compounds which as yet has no satisfactory explanation.

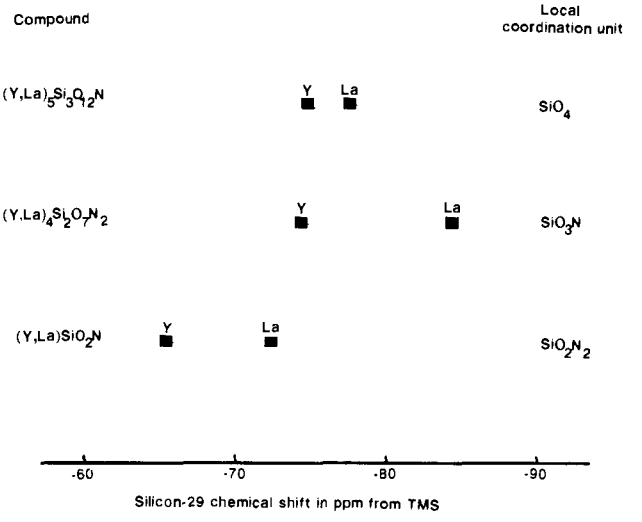

Figure 10. ^{29}Si isotropic chemical shift differences from isostructural compounds of the (Y,La)–Si–O–N systems.

^{27}Al MAS–NMR can also be used to identify phases and distinguish different local environments (e.g., AlO_6, AlO_4). However, subtle changes are often obscured by the incompletely averaged second-order quadrupole broadening, and some sites are broadened beyond detection. Quantitative detail is essentially lost because of the differential quadrupole broadening of the different sites which may prevent local models for compounds being distinguished by NMR and can produce a misleading impression of the phase distribution. To reduce these effects experiments on quadrupole nuclei should be performed at as high an applied field and as large a B_1 as possible in conjunction with small pulse angles. Understanding spectra from quadrupole nuclei is aided by performing experiments at more than one applied magnetic field if available. ^{139}La NMR will be of only limited use because of the extensive quadrupole broadening which allowed unequivocal interpretation of the data only for $LaAlO_3$, which has lanthanum in a closely cubic site.

(46) Bohm, J.; Fenkze, D.; Pfeifer, H. *J. Magn. Reson.* **1983**, *55*, 197–204.
(47) Janes, N.; Oldfield, E. *J. Am. Chem. Soc.* **1985**, *107*, 6769–6775.
(48) Dupree, R.; Smith, M. E. *Chem. Phys. Lett.* **1988**, *148*, 41–44.

Once a catalog of resonance positions associated with each phase has been established, this work has demonstrated that MAS-NMR (particularly ^{29}Si) is a powerful technique for examining ceramic phases. It can be used simply as a "finger-printing" technique to identify phases in complex phase mixtures, some of which were missed by conventional XRD analysis. MAS-NMR will give most advantage when mixtures of crystalline and glassy phases occur, and this is currently being investigated. MAS-NMR is an expanding field which will be increasingly used to probe ceramic systems.

Acknowledgment. We thank the SERC for support and a studentship (M.E.S.). We also thank Professor R. K. Harris for communication of his work prior to publication.

Biosynthetic Studies Using ^{13}C-COSY: The *Klebsiella* K3 Serotype Polysaccharide

David N. M. Jones and Jeremy K. M. Sanders*

Contribution from the University Chemical Laboratory, Lensfield Road, Cambridge, CB2 1EW U.K. *Received December 29, 1988*

Abstract: The biosynthesis of the *Klebsiella* K3 serotype polysaccharide has been elucidated by ^{13}C NMR spectroscopy of intact cultures under physiological conditions. Biosynthetic enrichment with [1-^{13}C]glucose suggested that the major biosynthetic pathway involved direct incorporation of the hexose moiety into the polysaccharide. A detailed analysis of the isotopomer distribution in the cross peaks of a phase-sensitive ^{13}C-COSY spectrum of polysaccharide biosynthetically labeled with [U-$^{13}C_6$]glucose revealed that approximately 30% of the glucose was catabolized prior to incorporation. Detailed analysis of the cross peaks in the phase-sensitive spectrum provided strong evidence that catabolism proceeds via the phosphogluconate pathway, a conclusion confirmed by the results of biosynthetic enrichment with [2-^{13}C]glucose.

^{13}C labeling for NMR spectroscopy has found widespread application in the elucidation of biosynthetic pathways in many organisms. However, the use of one-dimensional ^{13}C NMR spectroscopy is often limited in systems involving complex molecules. This complexity leads to crowded, overlapped spectra that are difficult to interpret. Recently Beale et al.[1] have developed triple-quantum-filtered INADEQUATE techniques to study the direct incorporation of [U-$^{13}C_3$]glycerol. We now show how ^{13}C-COSY spectroscopy can be used to obtain simultaneously information about intact and non-intact incorporation of ^{13}C-labeled precursors. In particular, we point out that the detailed information about the metabolic pathways involved in biosynthesis is contained in the isotopomer distributions which can be extracted from the multiplet patterns within the cross peaks of the COSY spectrum.

The appearance of cross-peak patterns in phase-sensitive COSY spectra is well understood. If A, M, and X are mutually coupled, then the cross peak between A and M has J_{AM} as the active coupling and J_{AX} or J_{MX} as the passive couplings. Lines separated by the active coupling appear antiphase, while those separated by a passive coupling appear in-phase. In ^1H-COSY spectra the observed nucleus is 100% abundant, with the result that all spins are coupled to all other adjacent spins and the cross peaks contain the full multiplets in both dimensions. Consequently there is no difference between the type of information available from the cross peaks in either dimension. This type of analysis is routine for ^1H-COSY spectra, including those of oligosaccharides.[2]

^{13}C-COSY spectra of biosynthetically labeled molecules are dramatically different, due to the appearance of additional multiplets within the cross peaks. The observed cross peaks are a combination of superimposed responses from molecules with different patterns of ^{13}C labeling. The presence of these additional components is attributable to substrate catabolism, which results in the loss of ^{13}C label at various sites. The appearance of these additional components can be used to analyze the substrate metabolism by exploiting the information provided by the active and passive coupling contributions to each cross peak. In the following discussion a shorthand notation for distinguishing between the cross peaks is adopted: the C-4, C-5 cross peak observed at δ C-4 in f_2 is represented as C^4_{45} with the corresponding cross peak at δ C-5 being represented as C^5_{45}.

The metabolic information available from COSY spectroscopy is illustrated for the *Klebsiella* K3 serotype polysaccharide that was biosynthetically labeled with specifically labeled glucose and universally labeled glucose as the carbon substrates. Labelling with [1-^{13}C]glucose showed that the major biosynthetic pathway for the polysaccharide incorporated the hexose moiety intact, while labeling with [U-$^{13}C_6$]glucose allowed us to acquire a ^{13}C-COSY spectrum and subsequently completely assign the one-dimensional ^{13}C NMR spectrum.[3] We show here that detailed analysis of the phase-sensitive cross peaks in the ^{13}C-COSY spectrum provides a powerful method for elucidating isotope distribution patterns and that, in this case, the pattern is consistent with a significant percentage of the glucose being catabolized through the phosphogluconate pathway prior to incorporation into the polysaccharide. These conclusions were confirmed by biosynthetically labeling the polysaccharide with [2-^{13}C]glucose and observing the predicted distribution of ^{13}C label in the resulting one-dimensional spectrum.

Results

The primary sequence (1) of the *Klebsiella* K3 serotype polysaccharide has recently been determined by Dutton and coworkers.[4] An initial spectrum was recorded at a low level of uniform labeling by using [U-14%-$^{13}C_6$]glucose (Figure 1a) and was found to be consistent with spectra recorded at the natural abundance level. The spectrum can be divided into four distinct regions: the carboxyl region (170-180 ppm), not shown but containing two resonances; the anomeric region (95-105 ppm), containing five well-resolved anomeric resonances; the ring region (60-80 ppm), containing 24 resonances with the lower field extreme corresponding to the glycosidically linked carbons and the

* Author to whom correspondence should be addressed.

(1) Beale, J. M.; Cottrell, C. E.; Keller, P. J.; Floss, H. G. *J. Magn. Reson.* **1987**, *72*, 574-578.
(2) Berman, E. *Eur. J. Biochem.* **1987**, *165*, 385-391.
(3) Jones, D. N. M.; Sanders, J. K. M. *J. Chem. Soc., Chem. Commun.* **1989**, 167-169.
(4) Dutton, G. G. S.; Parolis, H.; Joseleau, J.-P.; Marais, M.-F. *Carbohydr. Res.* **1986**, *149*, 411-423.

0002-7863/89/1511-5132$01.50/0